RHEOLOGY AND SETTLING DYNAMICS OF A PARTICLE FILLED AQUEOUS POLYMER GEL FOR HYDRAULIC FRACTURING FLUID SYSTEMS

Thesis

Presented in Partial Fulfillment of the Requirements for Graduation with Honors Research Distinction in the College of Engineering of The Ohio State University

By

Joseph A. Gauthier, B.S.

Chemical and Biomolecular Engineering

Ohio State University

2015

Thesis Committee:

Kurt W. Koelling, Advisor

Jacques Zakin

Abstract

Hydraulic fracturing, more commonly known as fracking, is a hydrocarbon capturing method that uses a high pressure fluid to fracture layers of shale, which then releases the hydrocarbons which flow to the surface for capture. In order to keep the fractures open, special sands called proppants are carried in with the fracking fluid. This functions by keeping the fracture open, while allowing natural gas to flow through the fracture. Hydroxypropyl Guar (HPG) is a high molecular weight, water soluble polymer used in the food industry as a viscosifier of water based foods, and in the petroleum industry as an additive in hydraulic fracturing fluids. The fracking fluid is further modified via addition of a cross linker, which causes the fluid to become a gel, making it extremely viscous.

Once the proppant is suspended in the fracture, a breaker is added to the solution which allows the fluid to flow again, while retaining the structure of the fracture. Unfortunately, some of the current fluid components used in industry are hazardous and present health risks upon unanticipated exposure.

This research aims to maintain, or surpass, current fluid standards by developing potential substitutes for the presently used components. To do this, a full factorial experimental design has been conducted with cross linker concentration and chopped nylon fiber concentration as exploratory variables. It is observed that the addition of the chopped fibers significantly decreases the settling velocity of suspended proppant particles, while not significantly affecting the fluid viscosity, thus allowing for a decrease in the toxic cross linker concentration for a given required settling velocity. Further, with rheological information, theoretical models will be developed for predicting settling velocities in a hypothetical fluid system.

Acknowledgements

I would like to thank my advisor, Dr. Kurt Koelling, for his guidance throughout my four years at Ohio State. Dr. Koelling has been instrumental in my success as a student and a researcher. I would also like to thank Nick Ohanian, Ziwei "Rocky" Wang, Xutao "Steve" Shi, Ann Maula, Tom Groseclose, and Jack Jones for their continued support throughout the work presented here.

Vita

2011 …….. Tippecanoe High School

2015 ……...… B.S. Chemical and Biomolecular Engineering, Ohio State University

2015 to Current ……. Ph.D. Chemical Engineering, Stanford University

Field of Study

Major Field: Chemical and Biomolecular Engineering

Table of Contents

Abstract iii
Acknowledgements iv
List of Figures vii
List of Tables vii
Introduction and Motivation 1
Chapter 1: Rheology 6
Introduction 6
Plan and Methods 7
Results and Discussion 9
Chapter 2: Settling Dynamics 18
Plans and Methods 18
Results and Discussion 20
Summary, Conclusions, and Future Work 27
References 30

List of Figures

Figure 1: Horizontal Frac, 2010 via Frac Focus, Creative Commons Attribution. 2
Figure 2: Importance of settling in fractures 3
Figure 3: Molecular structure of guar (Hercules Incorporated, 2007). 4
Figure 4: Crosslinking reaction between the guar backbone and the borate ion 4
Figure 5: SAOS experiment[15] 8
Figure 6: Ratio of bulk fluid viscosity containing fiber to fluid viscosity without fiber 10
Figure 7: Strain Sweep Results 11
Figure 8: G' as a function of frequency, cross linker (CL) concentration 12
Figure 9: Cross over frequency as a function of cross linker (CL) concentration 13
Figure 10: Complex viscosity as a function of frequency and CL concentration 13
Figure 11: General Viscoelastic Model Fitting 15
Figure 12: Shear viscosity vs shear rate 16
Figure 13: Cross Model fit to experimental shear viscosity data 18
Figure 14: Settling Dynamics Experimental Setup 19
Figure 15: Settling Velocity calculation 20
Figure 16: Settling velocity experimental data 21
Figure 17: JMP Analysis results 22
Figure 18: Stoke's Law modeling 24
Figure 19: Adjusted Stoke's Law Prediction 25
Figure 20: Power Law Prediction of Settling Velocity 26

List of Tables

Table 1: Full Factorial Experiment conducted 7
Table 3: Fitting Parameters in General Viscoelastic Model 15
Table 4: Fitting parameters for cross model 17
Table 2: PTFE sphere, Proppant properties 19
Table 5: Percent Error for adjusted Stoke's Law 25
Table 6: Percent Error for Power Law prediction of settling velocities 27

Introduction and Motivation

Hydraulic fracturing, more commonly known as fracking, is a process in which large quantities of high pressure fluid are used to fracture shale miles beneath the surface[1]. By doing this, the porosity and permeability of the rock are artificially enhanced, which allows hydrocarbons trapped in the shale to escape to the surface where they are captured and stored. However, once the fractures are created, if the pressure is released, the fractures will close. To mitigate this, special sands called proppants are suspended in water and injected into the well. With proppants placed in the fractures, the pressure can be released, as the proppants will prop open the fractures[1][2]. Thus the primary purpose of the fracking fluid is to allow these proppants to travel into the fracture. Figure 1, below, illustrates the overall fracking process.

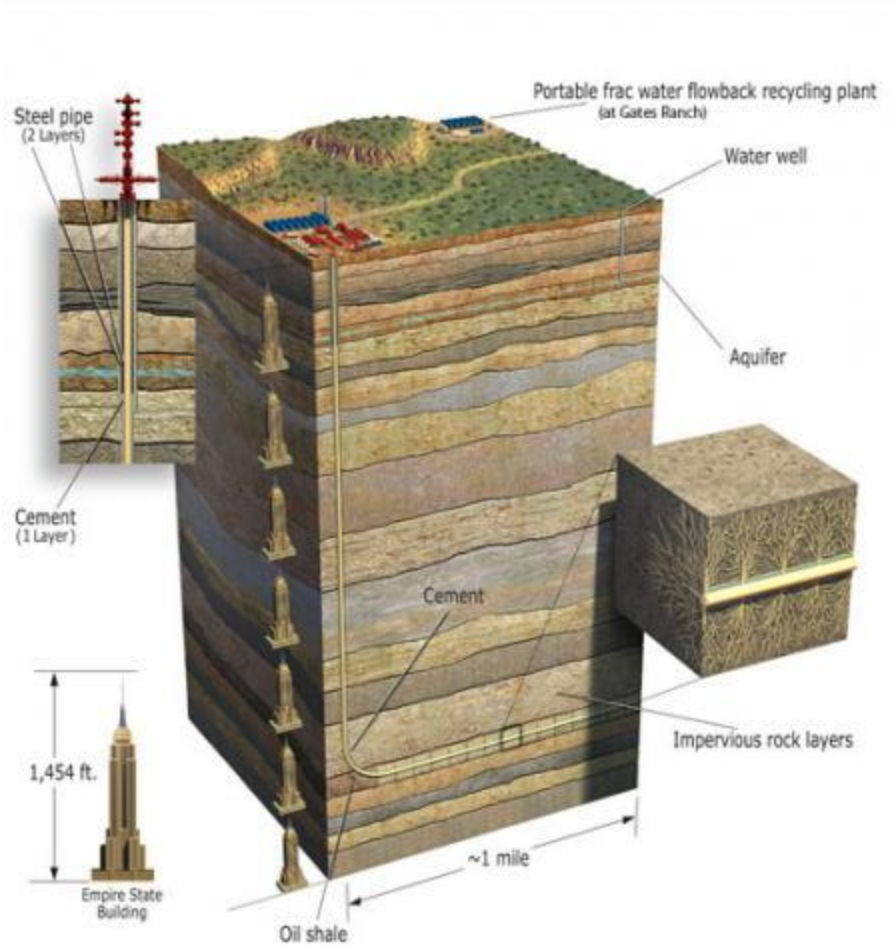

Figure 1: Horizontal Frac, 2010 via Frac Focus, Creative Commons Attribution.

As can be seen in the figure, the proppants must travel vertically into the fractures quite some distance. Since the sands are denser than water, it is necessary to increase the viscosity of the water used in hydraulic fracturing, so that the proppants do not settle to the bottom of the well. In this manner, a polymer called hydroxypropyl guar with molecular weight generally on the order of 10^5 to 10^6 is added to water as a viscosifier[3]. Figure 2 below illustrates the importance of settling velocity in hydraulic fracturing applications. The fluid must prevent proppant from settling out of the top portion of the fracture. To accomplish this, polymer and cross linker are typically added to the water and sand mixture.

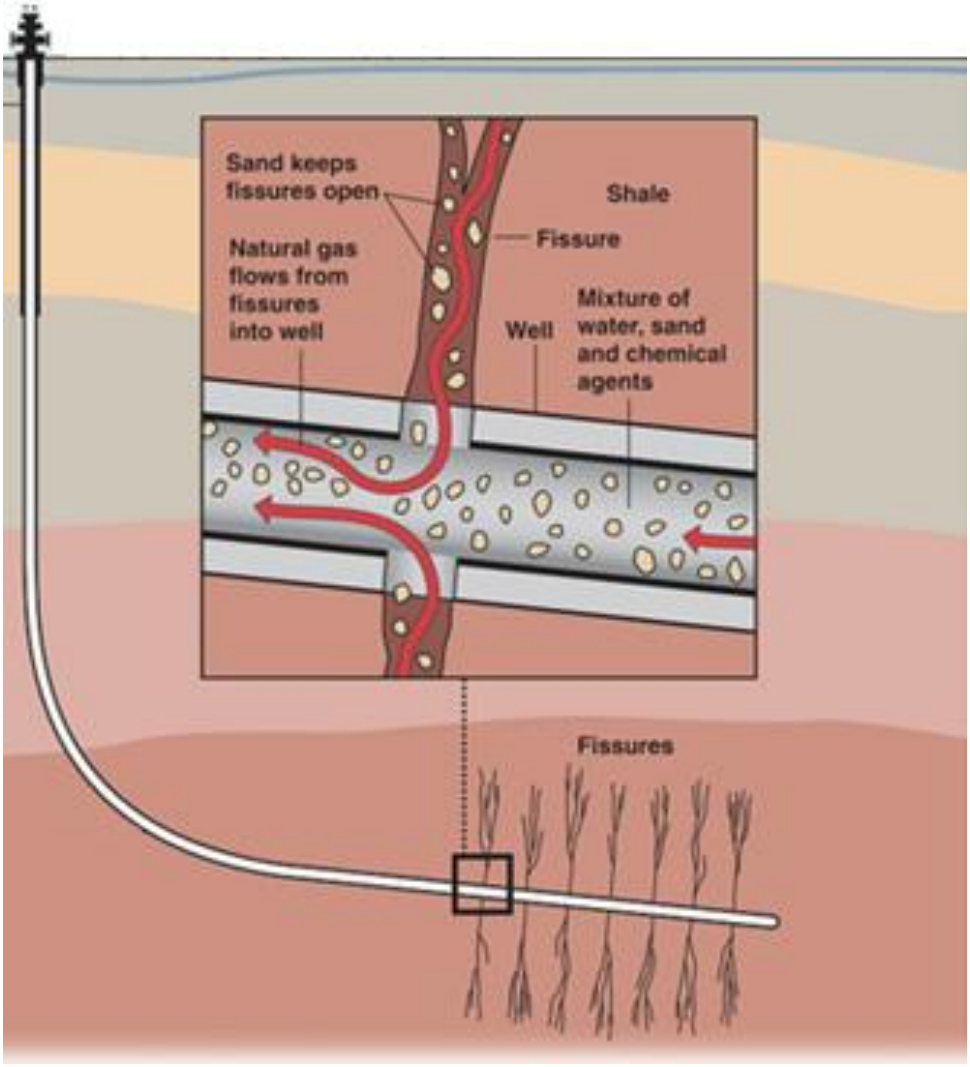

Figure 2: Importance of settling in fractures

As can be seen in Figure 3 below, the structure of guar resembles that of cellulose, which makes sense as it is derived from plant sources[4]. Guar has historically had uses in the food, textile, drag reduction, and paper industries, and was introduced into the oil industry during the 1960s as a potent viscosifier[4].

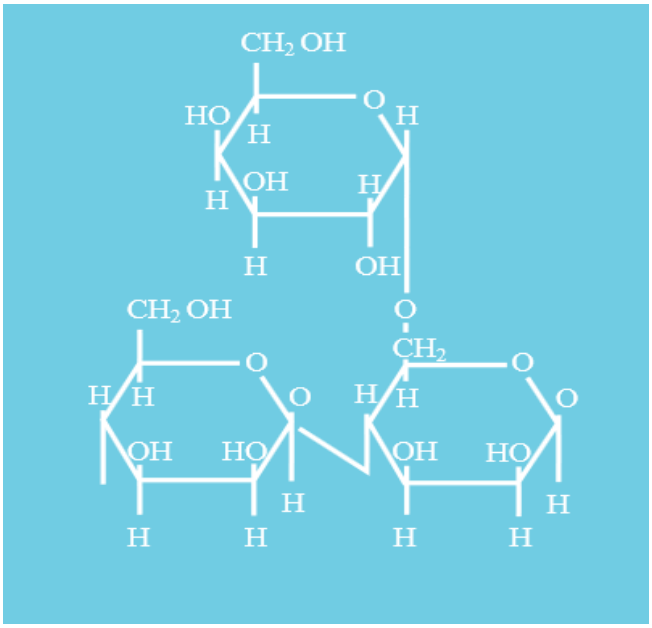

Figure 3: Molecular structure of guar (Hercules Incorporated, 2007).

To further increase the viscosity and proppant support of the fluid, the polymer chain is typically cross linked with metal compounds such as titanium, zirconium, or boron materials. These compounds react with the hydroxyl groups as seen above in the polymer chain, linking separate chains together, often at multiple segments along a single polymer chain[5]. Figure 4, shown below, further illustrates the cross linking process that sodium tetraborate, the cross linker of focus in this study, operates on.

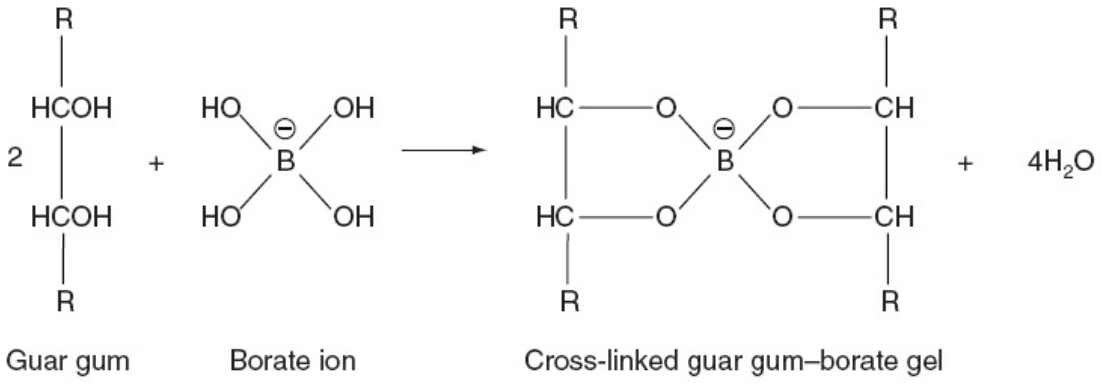

Figure 4: Crosslinking reaction between the guar backbone and the borate ion

Once the proppant has been placed in the well and the pressure released, the high viscosity fracking fluid must be pumped back to the surface to allow hydrocarbon capture. Since the viscosity of the fluid is very high, chemicals called breakers are added to the fracking fluid to reduce its viscosity. These breakers work by breaking the polymer backbone seen in Figure 3 above and are typically strong oxidizing agents such as ammonium persulfate[6].

Despite the large amounts of hazardous chemicals being used, hydraulic fracturing is widely performed in the United States and abroad because it produces enormous quantities of natural gas, the most environmentally friendly fossil fuel. More importantly, burning natural gas does not produce the notorious NO_x and SO_x commonly associated with burning coal, and it also produces far less CO_2 per unit energy produced compared to coal. Further, the United States is endowed with enormous amounts of shale containing natural gas, and in particular, the majority of eastern Ohio contains the Marcellus Shale[7]. Currently, 86% of natural gas produced in the United States comes from unconventional sources such as a hydraulic fracturing well, further illustrating the importance of hydraulic fracturing as an energy source in the US[1].

With this in mind, it is worth mentioning that hydraulic fracturing is certainly not without drawbacks. Many of the chemicals discussed above, in particular sodium tetraborate and ammonium persulfate, are quite hazardous at moderate concentrations. Further, the process of hydraulic fracturing was exempted from the Clean Water Act and the Safe Drinking Water Act in 2005[8][9]. These laws were designed to limit the quantity of chemicals that can be injected into drinking water aquifers, so in theory this allows gas and oil companies to inject unlimited quantities of chemicals into drinking water aquifers. However, in practice, all hydraulic fracturing wells use regulated casing technologies in the wells to prevent leaks from the drill bore into the aquifer[1].

Beyond the use of hazardous chemicals, hydraulic fracturing also uses enormous amounts of fresh water which is generally difficult to re-use or recycle after production, as many toxic components, such as radioactive ions picked up deep in the earth, cannot be easily removed[10]. Oil and gas companies have developed several strategies to deal with this waste water, such as injecting it into a depleted well, dump the waste water into

a lake or stream, treatment at a wastewater facility, or recycle the water into a new hydraulic fracturing well[11][12][1][8].

The goal of this research is to utilize rigid, chopped fibers in order to reduce the cross linker concentration required to maintain a given settling velocity of proppant in a hydraulic fracturing fluid. These fibers interact with the viscoelastic fluid by forming a network of rods that falling proppants must push out of the way or flow around to continue settling, thus ultimately reducing settling velocity[13][14].

Chapter 1: Rheology

Introduction

Rheological experiments such as small amplitude oscillatory shear, as well as high strain shear sweeps were performed on the viscoelastic polymeric samples in order to glean information about cross linking effectiveness, and the impact of adding fiber to the bulk fluid viscosity. Towards this end, two rheometers were used to investigate the rheological properties of the fluids. An ARES G-2 rheometer was used for the preliminary results, while an ARES LS-2 was used for the primary results presented in this work. These rheometers are very similar in form and function, and the switch was made only out of convenience of location.

As illustrated by Table 1 below, samples were prepared using a rigorous procedure to ensure repeatability, and were made in batches of four. First, enough water to make 400 g of base fluid was weighed using a mass balance. This water was added to a blender. Then, 2g of guar polymer obtained from Rhodia (JA GUAR 418, MW unknown but estimated to be $10^5 – 10^6$) was added to the blender, and the solution was blended gently for 30 seconds. The aqueous polymeric solution was then moved into a 500 mL jar and stirred gently at 150 RPM by a magnetic stirrer for one day so that foam and bubbles present in the polymer solution would equilibrate leaving just a polymer solution. Using a 100 mL graduated cylinder, the approximately 400 g polymer solution was split into four separate 500 mL jars, each with its own stir bar. Then, stirring vigorously at around 600 RPM, chopped nylon fiber (sourced from Patterson, L = 9.5 mm, D = 19 μm, L/D = 500) was very slowly added to ensure the fibers spread homogeneously throughout the sample.

If the sample was not selected to have fiber added, the samples were still stirred at 600 RPM for 5 minutes, or about the amount of time required to add fiber. Finally, again stirring vigorously at 600 RPM, cross linker (sodium tetraborate sourced from Fischer Scientific) was quickly added to ensure the cross linker could mix homogeneously throughout the sample before reacting, as mixing a cross linked gel is challenging. The samples were then stirred at 200 RPM overnight to ensure the reactions had proceeded to completion. At this point, samples were ready for experimentation.

Plan and Methods

A full factorial experiment was conducted measuring the rheological properties of hydraulic fracturing fluids. Four levels of cross linker concentration, four levels of fiber concentration, and one level of polymer concentration were explored. Cross linker concentration levels and the polymer concentration were chosen based on the industry standard, 0.08 wt %[13][5], while fiber concentration was selected based on preliminary results of the effective concentrations needed. Table 1 below illustrates the experimental design.

Table 1: Full Factorial Experiment conducted

Cross Linker Concentration (wt %)	Fiber Concentration (wt %)	Polymer Concentration (wt %)
0	0	0.5
0.04	0.02	
0.08	0.04	
0.12	0.08	

For each fluid sample prepared in this work, a strain sweep was performed to determine the viscoelastic limit of the material, such that the strain used in the frequency sweep would not enter the nonlinear viscoelastic regime. With this strain limit determined, three frequency sweeps were performed on the fluid, followed by two flow sweeps. All rheological plots presented in this work are the average of the two or three

experiments performed. It is worth noting that because these experiments do not take a long time to perform, evaporation was minimal and the results were very consistent from experiment to experiment.

In all of the experiments performed, a rotational rheometer (ARES LS-2 or ARES G-2) was used to rheologically characterize a material. The rheometer measures torque and the motor rotation rate simultaneously and accurately. In small amplitude oscillatory shear (SAOS) experiments, the motor imposes a small amplitude sinusoidal strain wave and measures the corresponding stress response of the fluid. This is illustrated below in Figure 5.

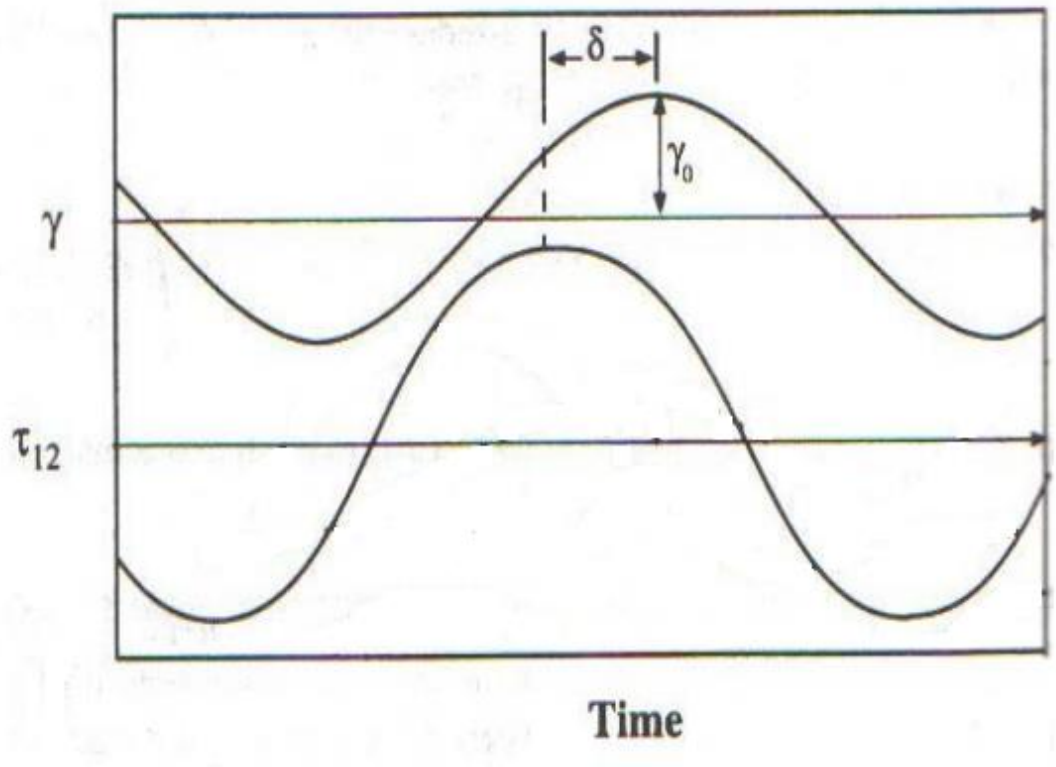

Figure 5: SAOS experiment[15]

As depicted in Figure 5, the strain wave, Equation 1, is imposed on a material, and the rheometer measures the shear stress tensor, $\tau_{12}(t)$, Equation 2. Generally the shear stress tensor will be shifted in time by a phase angle δ. This shear stress tensor can be decomposed into a

component perfectly in phase with the strain, and a component perfectly out of phase with the strain wave. The decomposed stress response is given by Equation 3, below.

$$\gamma(\mathrm{t}) = \gamma_0 * \sin(\omega * \mathrm{t}) \quad (1)$$

$$\tau_{12}(t) = \tau_0 * \sin(\omega * t + \delta) \quad (2)$$

$$\tau_{12}(t) = G' * \gamma_0 * \sin(\omega * t) + G'' * \gamma_0 * \cos(\omega * t) \quad (3)$$

G' is defined as the elastic or storage modulus, and is the portion of the stress response that behaves like a Hookean solid, while G'', the viscous or loss modulus, is the portion of the stress response that behaves like a Newtonian liquid. The relative magnitudes of these quantities give information about how solid like or how liquid like materials behaves at a given frequency and strain rate.

Another type of experiment performed in a rheometer presented in this work is a flow sweep, where a material is strained at a fixed strain rate, and the torque response measured can be used to calculate a shear stress. Thus at each strain rate a shear viscosity is measured as the shear stress divided by the strain rate. These experiments operate at extremely high strains and thus are generally the last experiment to be performed on a sample, as high strains tend to destroy structure in materials like gels.

Results and Discussion

Figure 6, shown below, illustrates that the addition of 0.08 wt % chopped fiber to cross linked fluids has a negligible effect on the bulk fluid viscosity. These preliminary results were performed at cross linker concentrations much higher than those seen in industry to exaggerate the effect of fibers on rheology and settling dynamics. This figure depicts the ratio of shear viscosity of the bulk fluid containing fiber to the bulk fluid containing no fiber. As can be seen, adding fiber has a negligible effect on bulk fluid viscosity, as most ratios range around 1. Further, it is worth noting that most rheological figures presented in this work will be presented on a log-log scale since rheological properties are generally extremely strong functions of variables like shear rate or concentration. However, even on a normal scale, the viscosity does not change much in

this case, further supporting the assertion that fiber does not increase viscosity by a significant amount.

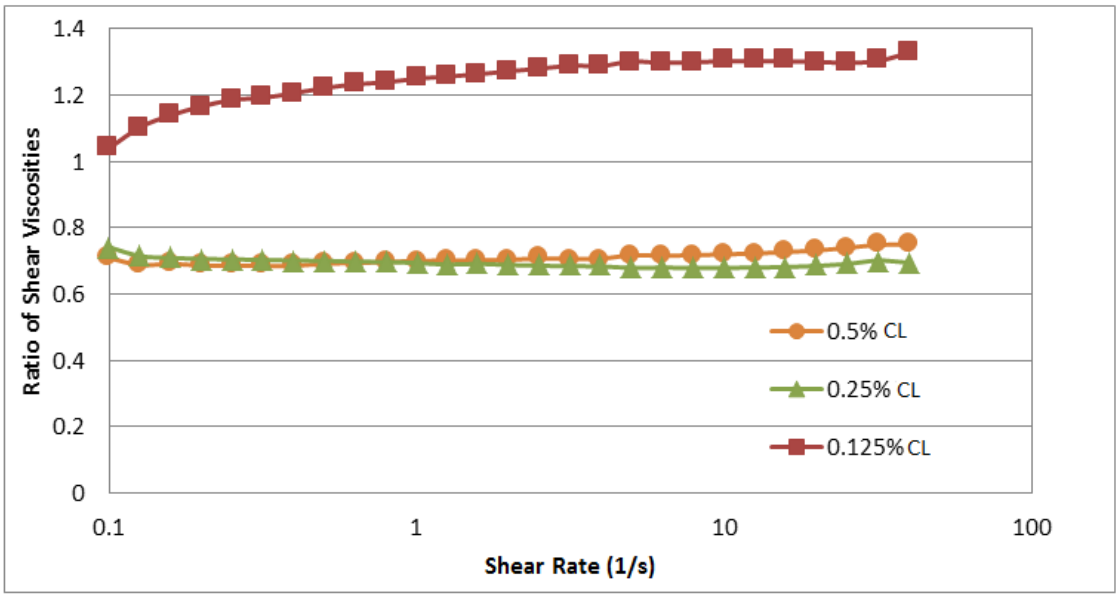

Figure 6: Ratio of bulk fluid viscosity containing fiber to fluid viscosity without fiber

With the fact that fiber has a negligible impact on rheological properties in mind, many rheological plots in this work will omit the fiber containing data, instead focusing on the experiments with fluids containing no fiber.

Figure 7, shown below, depicts the results of the strain sweep data obtained at a frequency of 1 rad/sec. As can be seen, the rheometer is unable to resolve noiseless data at strains below 2% as a consequence of the rheometer being strain controlled. Because the torque signals from the fluid are low with low strains, noise as a result of friction in the rheometer and vibrations from the environment contribute significant portions of the signal. At strains higher than 2%, the signal from the fluid dominates the noise signals and smooth curves for the elastic modulus result. The plots show a clear increase in the elastic modulus with cross linker concentration, as expected since the cross linker links together polymer chains. Further, at strains between 40-100%, the elastic moduli at all cross linker concentrations begin to decrease, indicating that the fluid is approaching a

nonlinear response. With this in mind, all frequency sweeps were performed at a strain of 10% so that a strong torque signal could be achieved while staying in the linear viscoelastic regime.

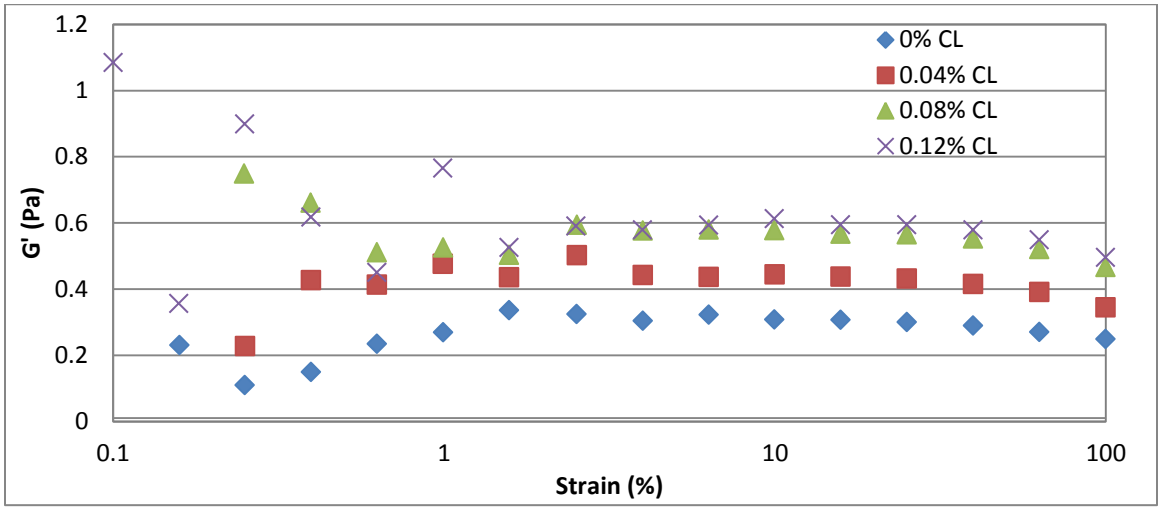

Figure 7: Strain Sweep Results

With the linear viscoelastic limit known, SAOS experiments were performed on the fracking fluids to determine how G' and G'' vary with frequency and cross linker concentration. As can be seen in Figure 8, at low frequencies, which correspond to longer length scales, the elastic modulus increases with increasing cross linker concentration. This is expected since adding cross linker increases the number of binding sites that the polymer chains experience and molecular bonds behave as Hookean solids. Further, at higher frequencies, which correspond to shorter length scales, the elastic modulus curves converge to roughly 10 Pa at 100 rad/sec. This is also expected since the materials tested are all similar, differing only in cross linker concentration. Thus, at extremely low length scales, the elastic moduli should be similar in magnitude as observed.

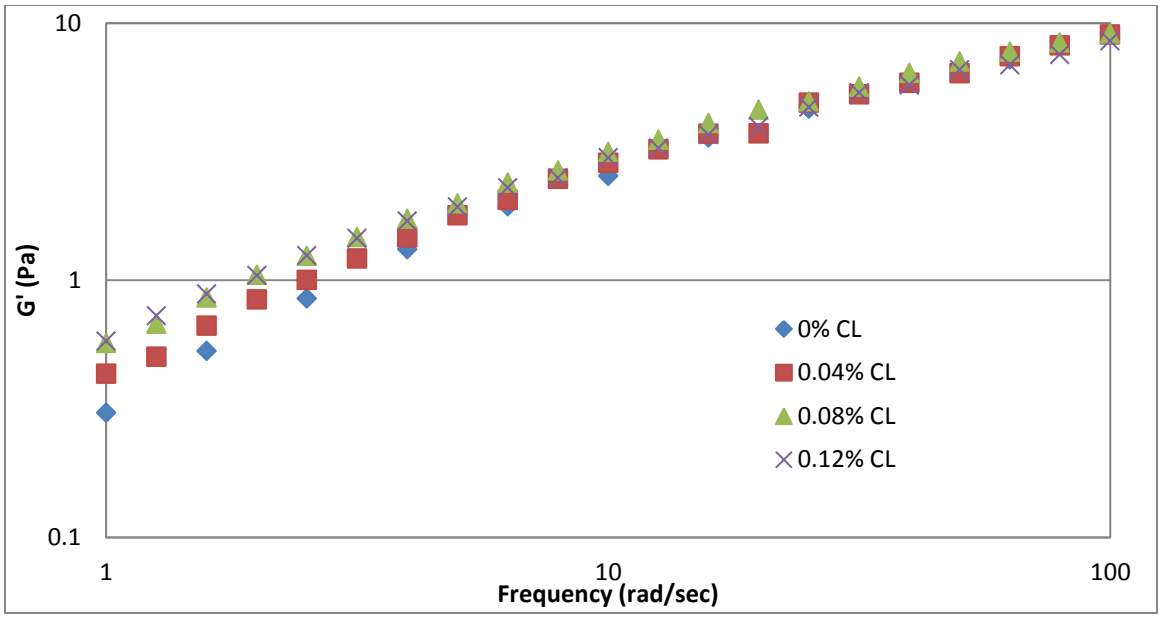

Figure 8: G' as a function of frequency, cross linker (CL) concentration

At low frequencies, most viscoelastic materials will exhibit a viscous modulus of larger magnitude than the elastic modulus since at large length scales most viscoelastic materials appear liquid like. With this in mind, the frequency at which the elastic modulus becomes larger than the viscous modulus can be informative as it describes the length scale at which the material becomes more solid-like than liquid like. Figure 9, below, illustrates this for the hydraulic fracturing fluid system. As can be seen, by increasing cross linker concentration, a lower cross over frequency is observed. This supports the idea that the cross linker acts by linking polymer chains together, since it is evidence that increasing cross linker increases the length scale at which the material begins behaving as an elastic solid.

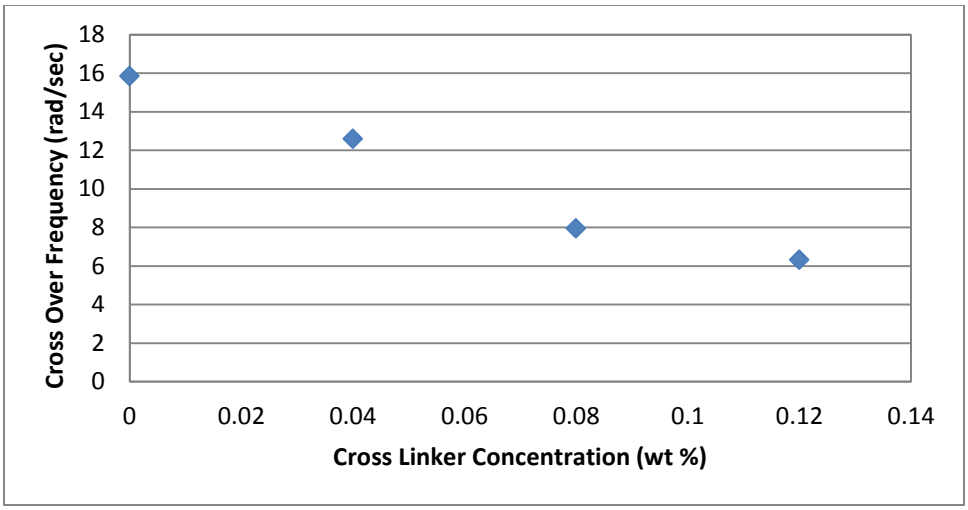

Figure 9: Cross over frequency as a function of cross linker (CL) concentration

A complex viscosity can be defined as a geometric mean of G', G'' divided by frequency. This definition is given by Equation 4, below. Further, a plot of complex viscosity as a function of frequency and cross linker concentration is given in Figure 10.

$$\eta^* = \sqrt{\left(\frac{G'}{\omega}\right)^2 + \left(\frac{G''}{\omega}\right)^2} \qquad (4)$$

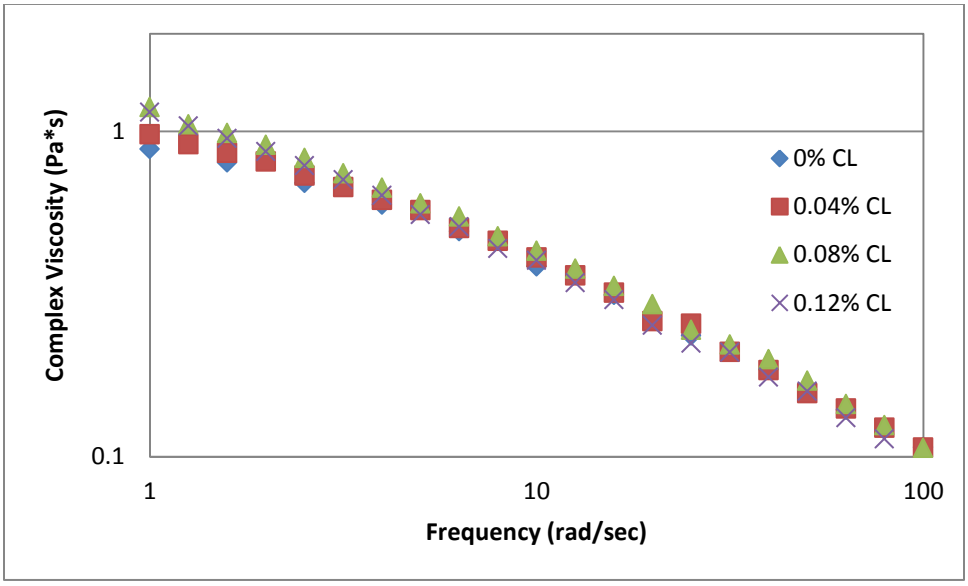

Figure 10: Complex viscosity as a function of frequency and CL concentration

The elastic and storage modulus can be modeled using the general viscoelastic model[15] given in Equations 5 and 6 below. As can be seen, this is a multi-mode model, with two fitting parameters, G_n and λ_n. In this work, a two mode model was used as it provided a good fit and so a higher mode model was not needed to describe the behavior observed.

$$G' = \sum_{n=1}^{\infty} \frac{G_n \omega^2 \lambda_n^2}{1 + \omega^2 \lambda_n^2} \quad (5)$$

$$G'' = \sum_{n=1}^{\infty} \frac{G_n \omega \lambda_n}{1 + \omega^2 \lambda_n^2} \quad (6)$$

The SAOS data were fit to the above model and the resulting prediction for complex viscosity as a function of frequency is shown below, along with the fitting parameters used in the above model. Table 2 shows the fitting parameters, and Figure 11 shows complex viscosity experimental data as points, with the model as solid lines.

As can be seen, the two mode model does an excellent job of fitting the data with four adjustable parameters per data set.

Table 2: Fitting Parameters in General Viscoelastic Model

	0% CL	0.04% CL	0.08% CL	0.12% CL
λ_1 (sec)	0.022	0.02	0.03	0.03
λ_2 (sec)	0.26	0.28	0.36	0.37
G_1 (Pa)	8.46	7.94	7.96	7.36
G_2 (Pa)	2.59	2.67	2.55	2.48

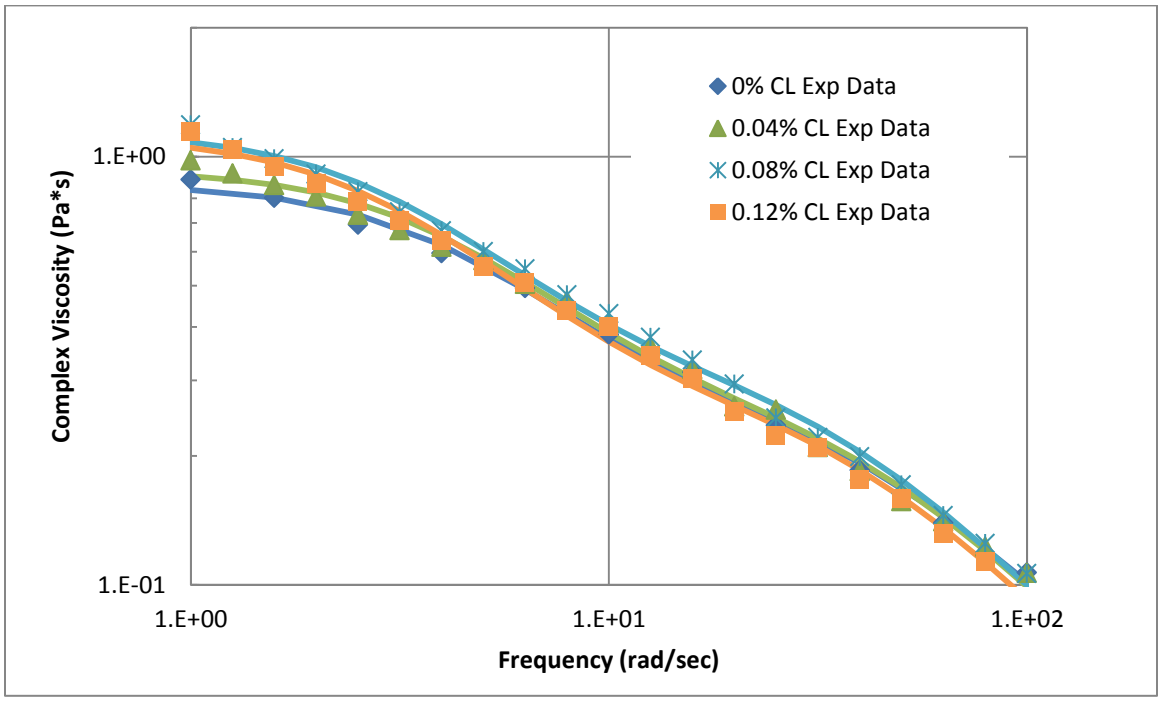

Figure 11: General Viscoelastic Model Fitting

Following the SAOS rheological experiments, high strain flow sweeps were performed to determine the shear viscosity as a function of shear rate. In this experiment, the rheometer fixes a strain rate and measures the torque response from which it calculates a shear stress. Once a steady state response is achieved, the shear viscosity is calculated by dividing the steady state shear stress by the strain rate. Figure 12, below, depicts the experimental data for this set of experiments.

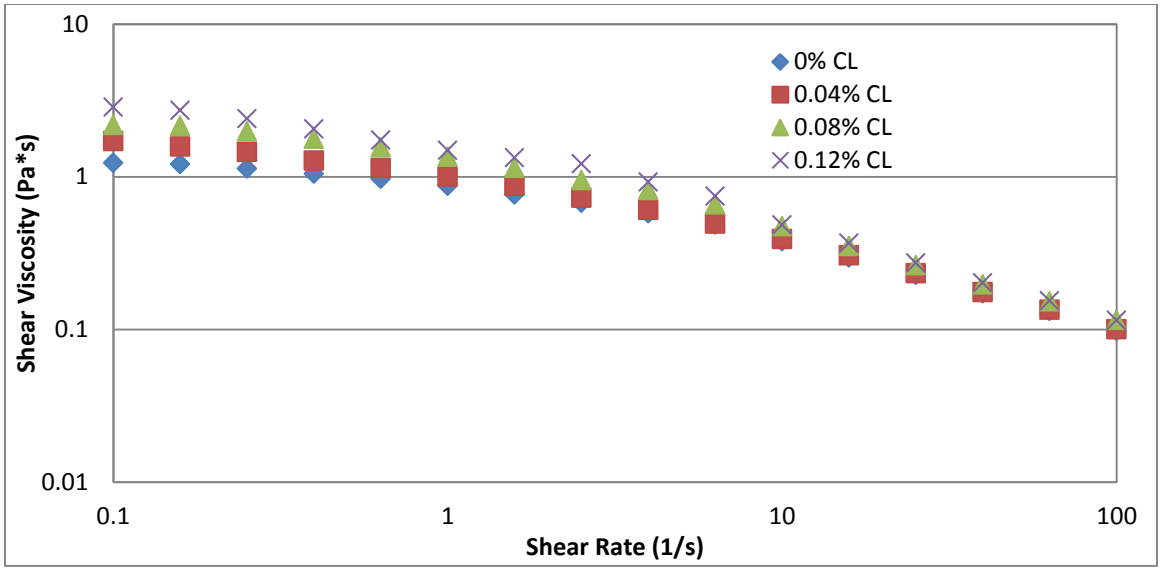

Figure 12: Shear viscosity vs shear rate

As can be seen in the plot, at low shear rate the viscosity increases significantly with increasing cross linker. This increase in viscosity, combined with the increase in elastic modulus observed in Figure 8, explains why companies add cross linker to hydraulic fracturing fluids – to significantly reduce settling velocity of proppant. Shear viscosity data can be effectively modeled with the Cross Model, given by Equation 7 below[15].

$$\eta = \eta_\infty + \frac{\eta_0 - \eta_\infty}{1 + (K * \dot{\gamma})^{1-n}} \qquad (7)$$

This model has four fitting parameters, namely η_0, η_∞, K, and n. η_0 is defined as the viscosity of the material as shear rate goes to zero, η_∞ is the viscosity as the shear rate goes to infinity, K and n are the flow parameters as determined in the more basic power law model. While this model has four fitting parameters, only three were experimentally fit. The infinite shear viscosity was set to the solvent viscosity, the viscosity of water. The parameters fit to the data are shown below in Table 3, and the resulting model fit is shown in Figure 13 below, where points are experimental data and the solid lines areteh model.

Table 3: Fitting parameters for cross model

	0% CL	0.04% CL	0.08% CL	0.12% CL
η_0 (Pa*s)	1.36	2.03	2.62	3.31
η_∞ (Pa*s)	1.0E-03	1.0E-03	1.0E-03	1.0E-03
K	0.41	0.97	0.86	1.06
n	0.31	0.36	0.30	0.28

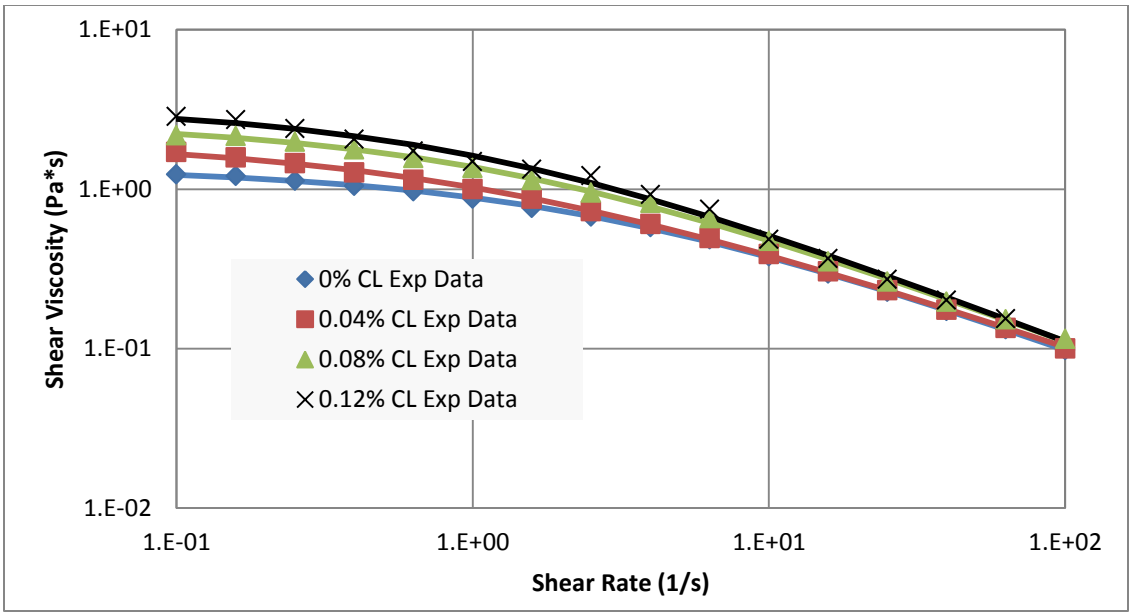

Figure 13: Cross Model fit to experimental shear viscosity data

As can be seen, the cross model does an excellent job of fitting the experimental shear viscosity data over all shear rates with three adjustable parameters and one known material parameter, the viscosity of water. In both the experimental data and the model, the shear viscosity for all cross linker cases converges at high shear rates. This is predicted by the cross model and is justified by noting that at infinite shear rate, the polymer molecules exhibit no entanglement and thus have minimal contribution to the viscous response of the material. This shear viscosity data will be used in a section to follow discussing modeling of settling velocity data is discussed.

Chapter 2: Settling Dynamics

Plans and Methods

At each level combination presented in Table 1, a settling rate was calculated by dropping a sphere made of polytetrafluoroethylene (PTFE) with diameter and density similar to that of a proppant particle through the fluid. A table comparing the properties of the PTFE sphere with proppant and an image of the experimental setup are shown below in Table 4 and Figure 14, respectively. The proppant particle was not used in the

settling rate experiments because the particles are too small for the camera to effectively track. Hence a larger particle of similar density was used.

Table 4: PTFE sphere, Proppant properties

	PTFE Sphere	Proppant
Density (g/mL)	2.2	2.0
Diameter (mm)	1.60	0.75

Figure 14: Settling Dynamics Experimental Setup

For each experiment, the PTFE particle was tracked using a camera. A 100 mL graduated cylinder was used as the testing apparatus, and the distance between 10 mL increments was known so that a settling velocity could be calculated. An "instantaneous" velocity was calculated between 80 and 70 mL, 70 and 60 mL, 60 and 50 mL, and finally

50 and 40 mL. These settling velocities were then averaged to give one data point as presented in this work. Avidemux video editing software was used to watch the video frame by frame so that settling times could be recorded to three decimal spots in seconds. Statistical calculations were performed using JMP software. Figure 15 below elucidates the velocity calculation process.

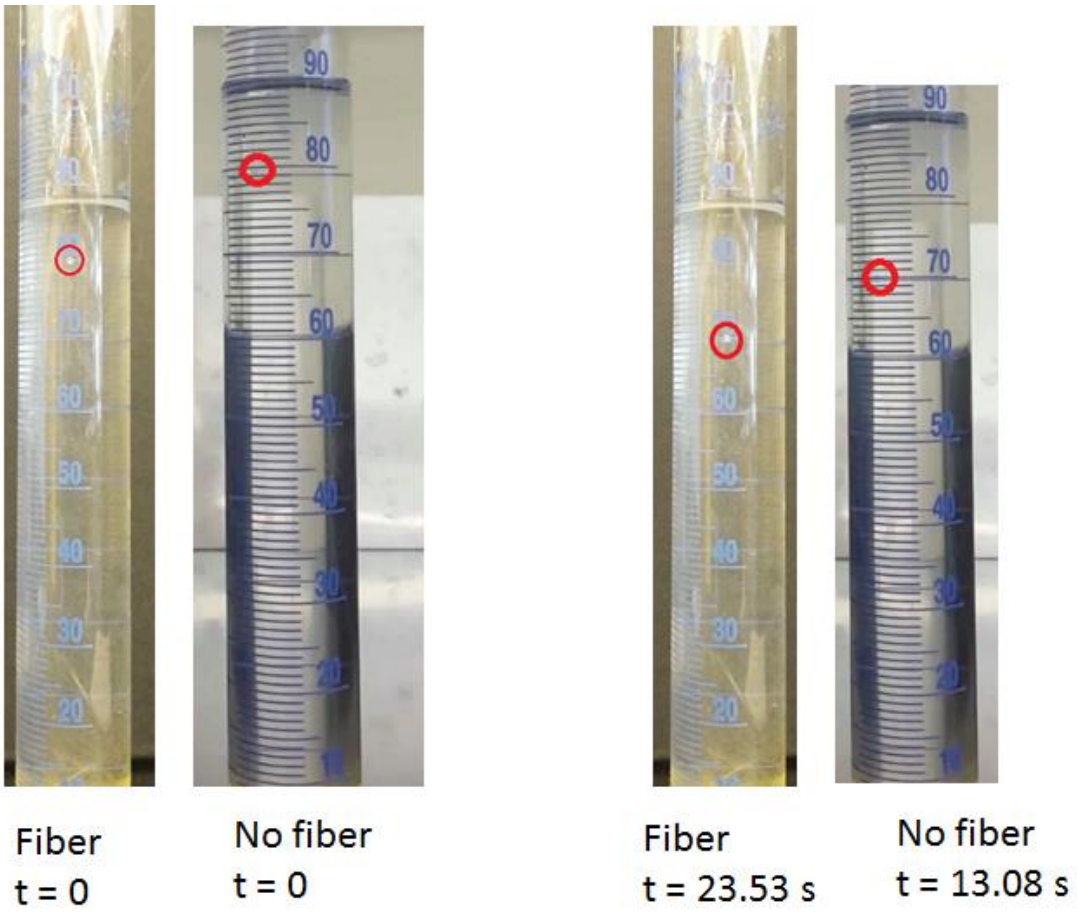

Figure 15: Settling Velocity calculation

Results and Discussion

As discussed in a previous section, a full factorial experiment exploring cross linker concentration and fiber concentration was performed, measuring settling velocity of a PTFE sphere through the hydraulic fracturing fluid. Each point in the design space was repeated once for a total of 32 settling rate experiments. Figure 16, below, illustrates the data from the 32 experiments. The repeated experiments were averaged to give a total of 16 data points.

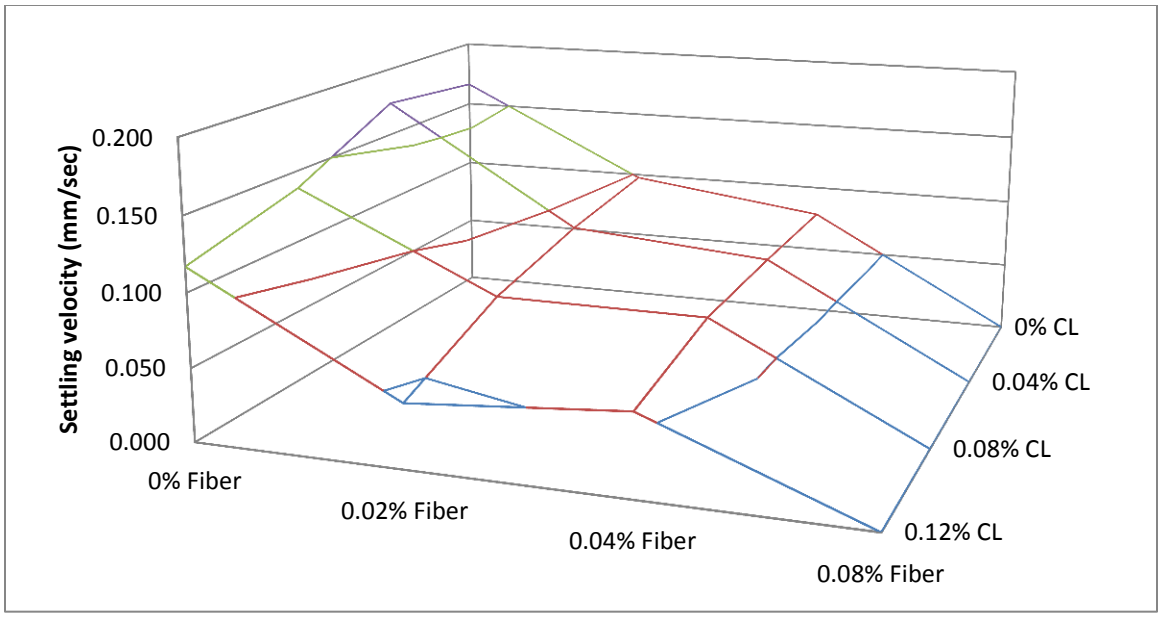

Figure 16: Settling velocity experimental data

As can be seen in the figure, both cross linker concentration and fiber concentration seems to have a significant effect on the settling velocity. At 0.08 wt% fiber, no settling is observed, even for the uncrosslinked case. The settling velocity data were statistically analyzed using the JMP software package. Using the fit model function of JMP, a model containing one linear term for cross linker concentration, one linear term for fiber concentration, and one linear term for a fiber-cross linker interaction term was fit to the settling velocity data. Figure 17, below shows a screenshot of the JMP analysis. Important values calculated by JMP are boxed in red.

Summary of Fit

RSquare	0.91
RSquare Adj	0.91
Root Mean Square Error	0.02
Mean of Response	0.07
Observations (or Sum Wgts)	32

Analysis of Variance

Source	DF	Sum of Squares	Mean Square	F Ratio	Prob > F
Model	3	0.09	0.03	100.13	$< 10^{-3}$
Error	28	0.01	0.00		
C. Total	31	0.10			

Parameter Estimates

Term	Estimate	Std Error	t Ratio	Prob > |t|
Intercept	0.15	0.01	24.07	1.00E-04
CL Conc	-0.27	0.07	-3.99	4.00E-04
Fiber Conc	-1.71	0.10	-16.65	1.00E-04
(CL Conc-0.06)*(Fiber Conc-0.03	6.24	2.30	2.72	1.12E-02

Effect Tests

Source	DF	Sum of Squares	F Ratio	Prob > F
CL Conc	1	4.71E-03	15.92	4.00E-04
Fiber Conc	1	0.08	277.08	1.00E-04
CL Conc*Fiber Conc	1	2.18E-03	7.37	1.12E-02

Figure 17: JMP Analysis results

As can be seen in Figure 17, the overall R^2 value for this model was greater than 0.9, meaning the model predicted more than 90% of the settling velocity variation observed. Further, the analysis of variance (ANOVA) test shows that the null hypothesis, that none of the factors have an effect on the response, is rejected with a p-value of less than 0.001, meaning at least one of the factors present has an effect on the response.

The more specific effect tests have a null hypothesis that allows testing whether an individual factor in the model has an influence on the response. As can be seen, all three terms in the model (fiber concentration, cross linker concentration, and the interaction term) all have a significant contribution on the model. Further, the effect of fiber is more significant than the effect of cross linker, as can be seen by the parameter

estimate. This result illustrates that, with statistical significance, fiber has an effect on the settling velocity of spheres through this hydraulic fracturing fluid.

The interaction term being significant along with its positive parameter estimate for settling velocity demonstrates that a synergy exists in the response settling velocity with fiber and cross linker concentration. That is to say, increasing fiber concentration and cross linker concentration has less of an effect on the settling velocity than the sum of the individual effects from increasing cross linker concentration and just increasing fiber concentration. This counter-intuitive result indicates that in designing a hydraulic fracturing fluid system, it is better to use all cross linker, or all fiber as the means for reducing settling velocity, ignoring economic reasons.

The settling data can be modeled using Stoke's Law, Equation 8 below. In this model, ρ_p is the density of the particle, ρ_f is the density of the bulk fluid, g is the gravitational constant, R is the radius of the particle, and η_0 is the viscosity of the bulk fluid. This model assumes that the flow around the spherical particle is perfectly laminar (low Reynolds Number), the fluid is Newtonian, and a homogeneous bulk fluid[15]. For the purpose of modeling these settling velocities, the viscosity of the fluid was chosen to be the zero shear viscosity as fit from the Cross model, since the particles settle slowly. Figure 18, below, shows the results of this modeling choice.

$$v_s = \frac{2}{9} * \frac{(\rho_p - \rho_f)}{\eta_0} * gR^2 \qquad (8)$$

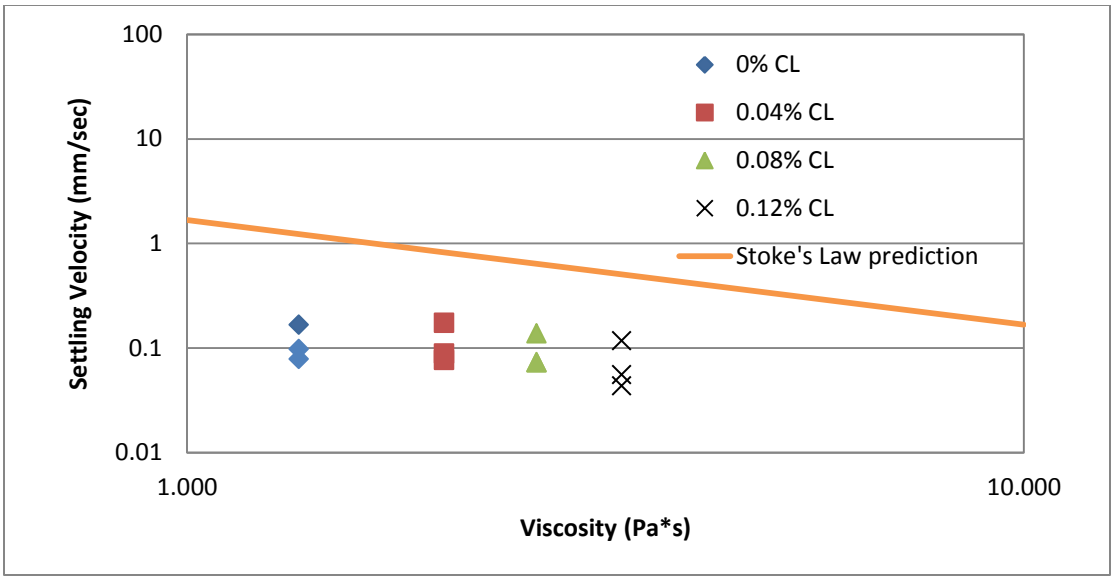

Figure 18: Stoke's Law modeling

In Figure 18, data points represent settling velocities measured while the solid line is the prediction from Stoke's law. The multiple points for each cross linker concentration represent varying fiber concentration, with 0.08% fiber omitted since it has a settling velocity of zero and the figure is on a log-log scale. As can be seen in the figure, Stoke's law does a poor job of predicting the settling velocities of the particles through a viscoelastic medium. This was not unexpected, since the fluids in question are very non-Newtonian and thus violate one of Stoke's Laws most important assumptions. However, Stoke's law forms an important base line for modeling. Further, the model does not take into account the contribution of the fibers inhibiting settling, which is clearly a significant factor.

A slight adjustment can be made to Stoke's law by using the fact that Stoke's law predicts a maximum shear rate given by Equation 9, below[16]. Figure 19, below shows the resulting prediction by Stoke's Law given the adjustment in shear rate and therefore viscosity. In this equation, v_s is the settling velocity and R_p is the particle radius.

$$\dot{\gamma}_{max} = \frac{3}{2} * \frac{v_s}{R_p} \qquad (9)$$

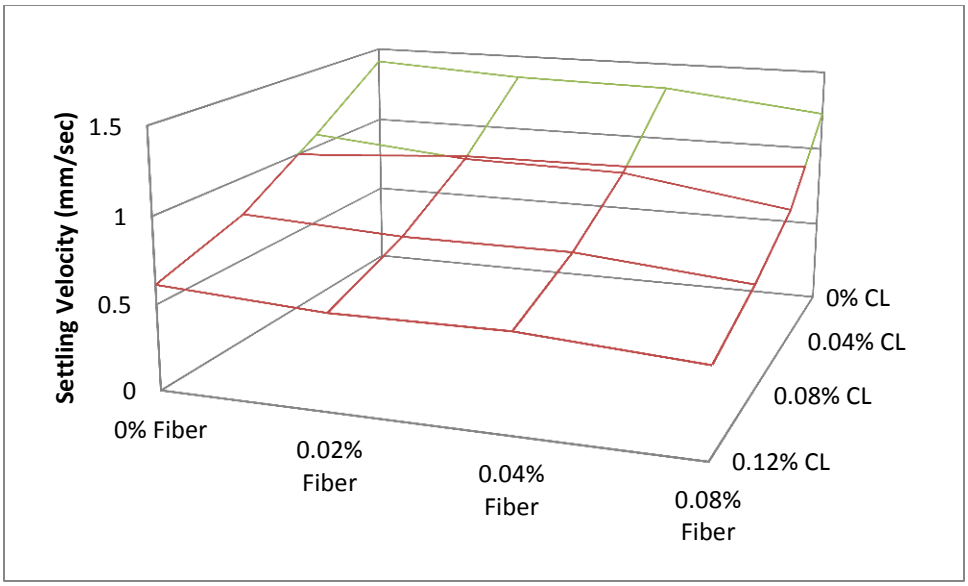

Figure 19: Adjusted Stoke's Law Prediction

As can be seen in the figure, the adjusted Stoke's law at least makes a correct qualitative prediction regarding settling rate as a function of cross linker and fiber concentration. However, as seen in Table 5 below, the prediction is still nearly an order of magnitude off from the observed settling velocity. Further, the use of this model requires already having observed the settling velocity in order to determine the shear rate, limiting its usefulness in practice.

Table 5: Percent Error for adjusted Stoke's Law

		Cross-Linker Concentration			
		0%	0.04%	0.08%	0.12%
Fiber Concentration	0%	88.2	83.9	82.3	80.9
	0.02%	92.8	91.1	90.0	92.2
	0.04%	94.1	92.1	90.0	90.3
	0.08%	NA	NA	NA	NA

A slightly more sophisticated model can be fit to the data by solving the equations of motion for a power law fluid. With this method, a particle Reynolds number must be defined, and is given by Equation 10 below[16].

$$Re_p = \frac{\rho_f * (v_s)^{2-n} * (R_p)^n}{K} \quad (10)$$

In this model, ρ_f is the fluid density, v_s is the settling velocity, R_p is the particle radius, and K, n are the flow index parameters given in Table 3. With a particle Reynolds number calculated, a predicted drag coefficient can be calculated and from the drag coefficient, a predicted settling velocity can be calculated[16]. The empirical drag coefficient and corresponding settling velocity are given in Equations 11 and 12 below, and a figure illustrating the model predictions is shown in Figure 20 below. In Equation 11, C_d is the drag coefficient. In Equation 12, m is the mass of the particle, g is the gravitational constant, and A is the projected area ($pi*R_p^2$).

$$C_d = \frac{35.2}{Re_p^{1.03}} + n\left(1 - \frac{20.9}{Re_p^{1.11}}\right)^{[16]} \quad (11)$$

$$v_s = \sqrt{\frac{2 * m * g}{\rho_f * A * C_d}} \quad (12)$$

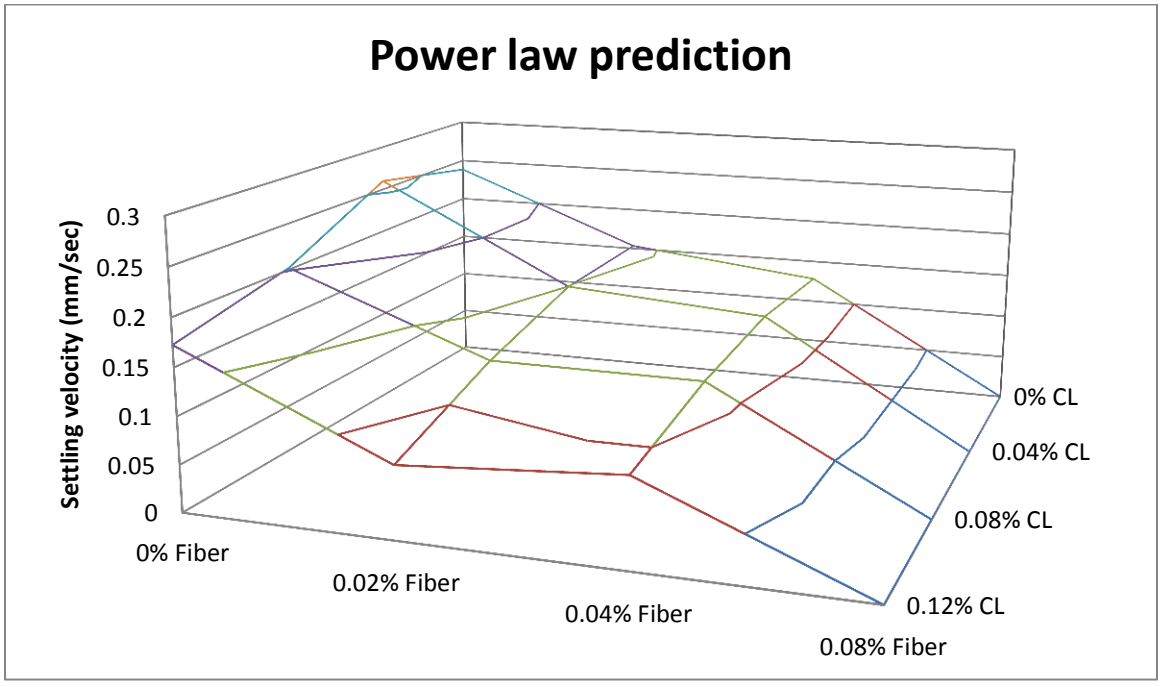

Figure 20: Power Law Prediction of Settling Velocity

As seen in Figure 20, the general shape is qualitatively correct, capturing the shape of the experimental data very effectively and is relatively close quantitatively. The 0.08% fiber prediction is zero because this model still requires a priori knowledge of the settling velocity to calculate the particle Reynolds number. The particle Reynolds number for all 0.08% fiber cases is zero, which leads to an infinite drag coefficient and therefore zero predicted settling velocity. The power law prediction does much better than the adjusted Stoke's model quantitatively, as seen in Table 6 below.

Table 6: Percent Error for Power Law prediction of settling velocities

		Cross-Linker Concentration			
		0	0.04	0.08	0.12
Fiber Concentration	0	43	49	47	47
	0.02	57	70	64	75
	0.04	64	75	64	68
	0.08	NA	NA	NA	NA

From the table, the model does reasonably well, within one half of an order of magnitude for the zero fiber case. However, as fiber concentration increases, the model begins to break down. Other more sophisticated models exist and follow the same pattern; they do well for the no fiber case and break down with adding fiber. This is because, as shown previously, the fiber adds a very significant drag contribution that viscosity alone cannot account for.

Summary, Conclusions, and Future Work

In this study, rheology and settling dynamics of a rod-like particle laden aqueous polymer gel related to hydraulic fracturing fluids was investigated. Rheological measurements gave insights to the relationship between stress and strain of the viscoelastic gels, and also elucidated the mechanism of cross linker on the polymer chains. At each cross linker concentration, a strain sweep, three frequency sweeps, and two flow sweeps were performed. It was shown that addition of chopped fibers to the

fluids has a negligible effect on the rheological properties of the fluid. Settling velocity experimentation gave a more direct measure of the performance of the hydraulic fracturing fluid, since the purpose of the fluid is to suspend proppant and prevent settling. Thus by measuring settling rate, we get an idea of how well a fracking fluid works.

As was clearly demonstrated by both the raw data and the statistical analysis, the addition of chopped fibers has a significant effect on the settling velocity of particles through the hydraulic fracturing fluid. Further, since the fiber cross linker interaction has a significant positive term in the statistical model, the combination of fiber and cross linker results in a faster settling velocity than just fiber or just cross linker, a surprising result. These two facts combined suggest that fiber could easily replace cross linker as a means to suspend proppant.

Beyond just the toxicity of the cross linker and the breaker required to break the cross linked fluid, another motivation to switching to just fiber is an economic argument. As can be seen in Figure 16, a fluid with 0% cross linker and 0.04% fiber has a slower settling velocity than the industry standard of 0.08% cross linker and 0% fiber. Further, as can be seen from Figure 13, the 0% cross linker fluid has a much lower viscosity than the 0.08% cross linker fluid, meaning the fluid would be easier to pump and would likely not need toxic breaker to assist in fluid production.

There is a clear need for the development of constitutive models that can predict the settling velocity of a sphere falling through a rod-like particle laden aqueous polymer gel, as none of the models investigated were effective at predicting settling velocity. Such a model would need to include terms that take into account the additional drag created by the presence of fibers as well as the shear thinning nature. As shown by the power law settling model, a shear thinning fluid generally will have a lower viscous drag portion of the total drag compared to a Newtonian fluid with zero shear viscosity equal to the zero shear viscosity of the shear thinning fluid. However, the fibers clearly add a very significant contribution to the total drag experienced by the particle, which sophisticated rheological models cannot predict with viscosity alone.

This work did not investigate the effect of the fiber properties, such as fiber diameter, length, aspect ratio, or modulus. It is suspected that these properties may play a major role in the effectiveness of the fiber in reducing settling velocity, and these topics are currently being investigated. In particular, mixing fibers into the fluid can be quite difficult. The nylon fibers used tended to bundle together in the fluid rather than disperse if they were mixed in too quickly. Thus if a hydrophobic fiber were to be used instead, mixing might be easier. Further, a bio-degradable fiber could be used so that the fiber would not damage pumping equipment at the producing end.

References

[1] Ground Water Protection Council and ALL Consulting, *Modern Shale Gas Development in the United States: A Primer*, 2009.

[2] "FracFocus," GWPC & IOGCC, 2014. [Online]. Available: fracfocus.org. [Accessed 7 November 2014].

[3] Halliburton, *Fracturing Fluid Systems: Broad Variety of Systems Enable Customizing the Treatment Fluid to Reservoir Requirements*, 2013.

[4] Hercules Incorporated, "Guar and Guar Derivatives Oil and Gas Field Applications," 2007. [Online]. Available: http://www.ashland.com/Ashland/Static/Documents/AAFI/PRO_250-61_Guar.pdf.

[5] R. Prud'homme, V. Constien and S. Knoll, *The Effects of Shear History on the Rheology of Hydroxypropyl Guar Gels*, Polymers in Aqueous Media (vol 223*)*, 1989, pp. 89-112.

[6] M. Sarwar, K. Cawiezel and H. Nasr-El-Din, *Gel Degradation Studies of Oxidative and Enzyme Breakers to Optimize Breaker Type and Concentration for Effective Break Profiles at Low and Medium Temperature Ranges*, Society of Petroleum Engineers, 2011.

[7] U.S. Energy Information Administration, *United States shale gas plays*, 2011.

[8] A. Andrews, P. Folger, M. Humphries, C. Copeland, M. Tiemann, R. Meltz and C. Brougher, Unconventional Gas Shales: Development, Technology, and Policy Issues, Darby: Diane Publishing Co., 2010.

[9] 109th Congress of the United States of America, Washington D.C., 2005, p. 101.

[10] J. D. Arthur, B. K. Bohm and D. Cornue, *Environmental Considerations of Modern Shale Gas Development*, Society of Petroleum Engineers, Jan. 2009.

[11] M. Zoback, S. Kitasei and B. Copithorne, *Addressing the Environmental Risks from Shale Gas Development*, WorldWatch Institute, Vol 21, 2010.

[12] E. Barbot, N. Vidic, K. Gregory and R. Vidic, *Spatial and Temporal*

Correlation of Water Quality Parameters of Produced Waters from Devonian-Age Shale following Hydraulic Fracturing, Vol. 47, American Chemical Society, 2013, pp. 2562-2569.

[13] R. Barati and J.-T. Liang, *A Review of Fracturing Fluid Systems Used for Hydraulic Fracturing of Oil and Gas Wells,* Journal of Applied Polymer Science, Vol. 131, 2014.

[14] C. Bivins, C. Boney, C. Fredd, J. Lassek, P. Sullivan, J. Engels, E. Fielder, T. Gorham, T. Judd, A. Sanchez Mogollon, L. Tabor, A. Munez and D. Willberg, *New Fibers for Hydraulic Fracturing*, Vol. 17, Schlumberger Limited, 2005.

[15] C. W. Macosko, Rheology Principles, Measurements, and Applications, Hoboken: Wiley-VCH, 1994.

[16] Graham, D., & Jones, T. (n.d.). *Settling and transport of spherical particles in power-law fluids at finite Reynolds number*. Journal of Non-Newtonian Fluid Mechanics, Vol. 54, 1994, pp. 465-488.